Journal of Sound and Vibration (2002) **254**(1), 143–162
doi:10.1006/jsvi.2002.4090, available online at http://www.idealibrary.com on IDEAL®

RELIABILITY ANALYSIS OF SUSPENSION BRIDGES AGAINST FLUTTER

S. POURZEYNALI

Department of Civil Engineering Faculty, Guilan University, Rasht, Iran

AND

T. K. DATTA

Department of Civil Engineering, Indian Institute of Technology, Delhi, Hauz Khas, New Delhi 110 016, *India. E-mail: tkdatta@civil.iitd.ernet.in*

(*Received* 3 *April* 2001, *and in final form* 5 *September* 2001)

A reliability analysis of suspension bridges against flutter failure is presented using the basic theory of reliability. For the purpose of analysis, uncertainties considered are those arising from the variations in geometric and mechanical properties of bridge, modelling, damping and experimentally obtained flutter derivatives. These uncertainties are incorporated by multiplying the computed flutter wind speed with a number of independent factors, which are considered as random variables. Each factor is assumed to follow log-normal distribution. The wind environment at the site, which may cause flutter failure, is considered as the other uncertainty necessary for computing the reliability against flutter failure. The flutter wind speed for the bridge is determined using a finite element approach and a multimode analysis. The effect of some important parameters such as the mean wind speed at the site, coefficients of variation of the multiplying factors associated with damping, modelling and flutter derivatives on the reliability estimates is investigated. The results of the study show that the reliability against flutter failure is sensitive to the variation of the above parameters.

1. INTRODUCTION

Most of the studies of wind-induced vibration of suspension bridges relate to the determination of the flutter wind speed and buffeting response of the deck. The developments of flutter and buffeting analysis of flexible and long-span cable-supported bridges (suspension and cable stayed bridges) under wind forces owe much to the studies of Davenport [1, 2], Lin [3], Scanlan and Gade [4], Bucher and Lin [5], Nakamura and Yoshimura [6], and Scanlan and Jones [7]. In the recent past, several investigations concerning the response of cable-supported bridges to wind-induced vibration have been performed [8–10]. Responses have been obtained by time domain analysis [11] and also by frequency domain analysis [7, 12]. The studies also included wind tunnel tests on scaled models [13, 14]. In 1996, Jain *et al.* [15] carried out a comprehensive study on the coupled flutter and buffeting analysis of long-span bridges by a continuum approach and by using spectral analysis technique. The same concept was extended by Katsuchi *et al.* [16] to obtain the multimode coupled flutter and buffeting analysis of the Akashi-Kaikyo Bridge in Japan. This study showed a good agreement between the wind tunnel test results and those of the theoretical analysis.

0022-460X/02/$35.00

Compared to the dynamic response analysis of suspension bridges, reliability analysis of suspension bridges against dynamic phenomena is relatively less. Malla [17] presented a reliability analysis of cable stayed bridges for seismic forces. Henrik *et al.* [18] carried out a study on the reliability analysis of the East Bridge across the Great Belt in Denmark, against flutter wind speed. The study was done on the basis of measuring the critical wind speed values on a scale model in wind tunnel tests. The considered uncertainties mostly related to the conversion from model to the prototype, and to the structural damping. Apart from this work, no other study in finding the reliability of suspension bridges against flutter failure is reported in the literature. Since the flutter wind speed of suspension bridges is an important consideration in its design, it is desirable that the reliability of such bridges against flutter condition should be properly evaluated.

Wind-induced flutter in suspension bridges is a complex phenomenon involving many issues like bridge geometry, wind direction, modeling of the bridge and flutter derivatives, etc. However, using simplified assumptions, flutter wind speed of suspension bridges has been obtained by several investigators which have been referred to in the preceding paragraphs.

In line with these assumptions, the reliability of a suspension bridge against flutter speed is presented here using the reliability analysis technique. For the purpose of analysis, geometric and mechanical properties of the bridge, modelling, damping and the flutter derivatives are considered as uncertainties. These uncertainties are also assumed to be log-normally distributed. The wind environment at the site is considered as the other uncertainty which is used for the reliability against flutter failure of the bridge. A parametric study is conducted to show the effect of some important parameters on the reliability against flutter. They include mean wind speed at the site, and coefficients of variation of the parameters influencing the computation of flutter wind speed.

2. ASSUMPTIONS

The following assumptions are made in the analysis: (1) all stresses in the bridge elements obey the Hooke's law, and therefore no material non-linearity is considered; (2) the initial dead load is carried by cables without causing any stress in the suspended structure; (3) the cable is assumed to be of a uniform cross-section and of a parabolic profile under dead load such that the weight of the cable can be assumed to be uniformly distributed along the span instead of along the length of the cable; (4) the hangers (or suspenders) are assumed to be vertical and inextensible, and their forces are considered to be distributed loads as if the distance between the suspenders were very small; (5) the original shape of every cross-section of the bridge deck is unaltered during vibration although the section may undergo out-of-plane deformation (warping). Also, the peripheral bending in the walls of the section is negligible; (6) it is assumed that there is no tower resistance to displacement at the tower top and so the horizontal components of the cable tension H_w, (due to dead load) and $H(t)$, (due to dynamic load) are the same on both sides of the tower.

3. FREE VIBRATIONAL ANALYSIS

For the dynamic analysis of suspension bridges, both 3-D and 2-D idealizations have been used in modelling the structure. 3-D modelling has been adopted mostly for finite element analysis in which suspension system, the deck and piers are all taken together as an integrated structure [19]. 2-D modelling has been adopted for both continuum method and finite element method (FEM) of analysis. It has been observed that 2-D modelling provides

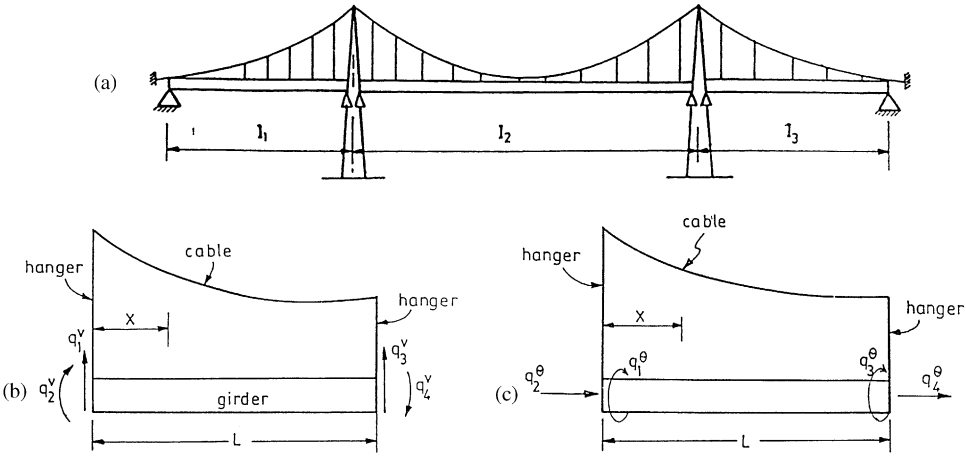

Figure 1. (a) Suspension bridge model; (b) bridge element with vertical displacement; (c) bridge element with torsion.

sufficiently accurate natural frequencies and mode shapes for the vertical and torsional vibrations of the bridge deck [20, 21]. In the present analysis, a 2-D FEM modelling using lumped mass matrix has been adopted for finding the mode shapes and frequencies. For this purpose, the bridge deck is idealized as a beam element having bending and torsional degrees of freedom. At each node, the kinematic degrees of freedom considered are shown in Figures 1 (b, c). The dynamic degrees of freedom at the nodes are considered as the vertical and torsion (Sant-Venant) degrees of freedom only; the rotational and warping degrees of freedom are condensed out. Since bending and torsional vibrations are uncoupled in free vibration of suspension bridges, the torsional and (vertical) bending modes are obtained separately. This modelling and analysis techniques lead to certain approximations which are well accepted in the literature for the free vibration analysis of suspension bridges.

The equation of motion for the free vibrating suspension bridge in bending mode is derived by calculating the total potential and kinetic energies of the system and by applying the *Hamilton's principle*. The bridge is divided into a system of discrete elements. Each element consists of bridge deck and cable connected by at least two hangers as shown in Figure 1(b). The shape functions of the element are assumed to be cubic Hermitian polynomials. The displacement vector of the element can be expressed as

$$v_e(x, t) = \{f^v(x)\}_e^{\mathrm{T}} \{q^v(t)\}_e \tag{1}$$

in which $\{q^v(t)\}_e$ is the nodal displacement vector of the element; $\{f^v(x)\}_e^{\mathrm{T}}$ is the vector of the shape functions. Considering the total energy of the system to be consisting of (1) strain energy and gravity energy of the cables, (2) potential energy of the deck and (3) kinetic energy of the system, the elemental equilibrium of the system can be derived by minimizing the total energy of the system [20]. This leads to an elemental stiffness matrix corresponding to the degrees of freedom shown in Figure 1(b). The elemental stiffness matrices are assembled to from the overall stiffness matrix. Since vertical degrees of freedom are considered only as the dynamic degrees of freedom for bending vibration, the overall stiffness matrix described above is condensed to retain only the dynamic degrees of freedom. The equation of motion for undamped free vibration can be then written in the following form:

$$[\mathbf{M}^V]\{\ddot{r}^V\} + [\mathbf{K}^V]\{r^V\} = \{0\}, \tag{2}$$

where $\{r^V\}$ is the nodal displacement vector containing vertical degrees of freedom only, $[\mathbf{K}^V]$ is the condensed stiffness matrix; and $[\mathbf{M}^V]$ is the lumped mass matrix of the system respectively. Solution of the free vibration equation provides the natural frequencies and mode shapes of the bridge.

For the torsional vibration of the suspension bridge, the governing equation of motion can be obtained in a similar way as that obtained for the vertical vibration. In this case, as shown in Figure 1(c), q_1^θ and q_3^θ are the torsional rotations, and q_2^θ and q_4^θ are the warping displacements of the bridge element. The warping displacements are condensed out as described for the bending vibration.

The equation of motion for torsional vibration takes the form

$$[\mathbf{M}^\theta]\{\ddot{r}^\theta\} + [\mathbf{K}^\theta]\{r^\theta\} = \{0\} \tag{3}$$

in which $[\mathbf{M}^\theta]$ is the lumped mass moment of inertia; and $[\mathbf{K}^\theta]$ is the overall stiffness matrix of the system, respectively, and $\{r^\theta\}$ is the torsional degrees of freedom at the nodes. Solution of equation (3) provides the torsional mode shapes and frequencies. Since vertical and torsional modes of vibration are uncoupled in free vibrations, as described, equations (2) and (3) are shown separately to obtain the structural frequencies in vertical and torsional vibrations. During flutter condition, coupling between vertical and torsional modes of vibration takes place due to aerodynamic effects. As a result, the equation of motion for flutter contains both vertical and torsional degrees of freedom as shown later in equation (6).

4. EQUATION OF MOTION IN FLUTTER

The bridge deck is discretized into two-dimensional beam elements each consisting of two nodes at its ends. At each node, two degrees of freedom, vertical displacement and torsional rotation are considered.

The wind-induced aeroelastic or self-excited forces can be lumped at both ends of each element as shown in Figures 2(c) and (d). The aeroelastic forces per unit length of the bridge are given by Jain *et al.* [15] as

$$L_e = \frac{1}{2}\rho U^2 B\left[kH_1^*\frac{\dot{h}}{U} + kH_2^*\frac{B\dot{\theta}}{U} + k^2H_3^*\theta + k^2H_4^*\frac{h}{B}\right], \tag{4}$$

$$M_e = \frac{1}{2}\rho U^2 B^2\left[kA_1^*\frac{\dot{h}}{U} + kA_2^*\frac{B\dot{\theta}}{U} + k^2A_3^*\theta + k^2A_4^*\frac{h}{B}\right] \tag{5}$$

in which L_e and M_e are the aeroelastic vertical lift force and torsional moment of the element per unit length, respectively, ρ is the air mass density; U is the mean wind velocity; B is the bridge deck width; $k = B\omega/U$ is the reduced frequency; ω is the circular response frequency; H_i^* and A_i^*, $i = 1$–4 are functions of k and are the experimentally determined flutter derivatives for the deck cross-section under investigation. h and θ are the vertical displacement and torsional rotation at the nodes of the bridge element respectively. Overdots indicate the time derivative. The distributed aeroelastic forces are considered to be constant along the element.

The governing equation of motion in the matrix form can be expressed as

$$[\mathbf{M}]\{\ddot{x}\} + [\mathbf{C}]\{\dot{x}\} + [\mathbf{K}]\{x\} = \{F\}, \tag{6}$$

where $[\mathbf{M}]$, $[\mathbf{C}]$ and $[\mathbf{K}]$ are the mass, damping and stiffness matrices, corresponding to both vertical and torsional degrees of freedom; $\{F\}$ is the $(2n \times 1)$ vector of aeroelastic forces;

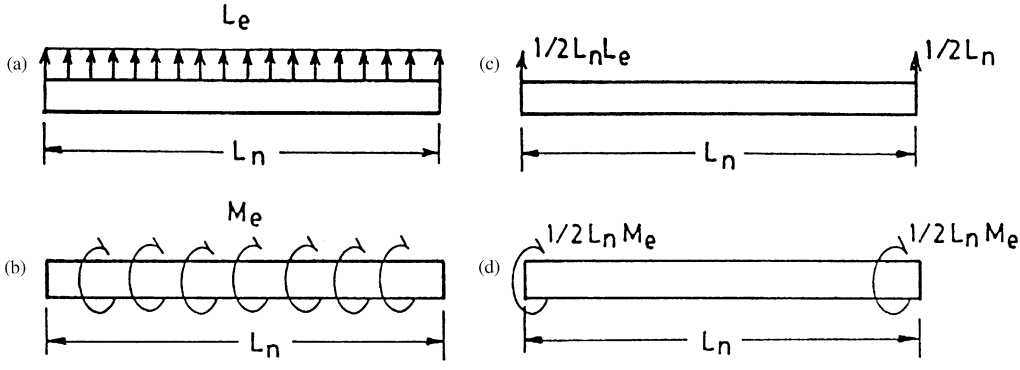

Figure 2. Self-excited forces: (a) distributed vertical load; (b) distribution torsional moment; (c) lumped vertical load; (d) lumped torsional moment.

and $\{x\}$ is the $(2n \times 1)$ response vector defined as

$$\{x\} = \{h_1, h_2, \ldots, h_n, \theta_1, \theta_2, \ldots, \theta_n\}^{\mathrm{T}}_{1 \times 2n} \tag{7}$$

in which n is the number of nodes along the total bridge length; h_i and θ_i are the vertical and torsional displacement at the ith node respectively.

Using equations (4) and (5), the $(2n \times 1)$ aeroelastic force vector $\{F\}$ can be expresed in the form

$$\{F\} = \frac{1}{2}\rho U^2 B\left(\frac{k}{U}\right)[\mathbf{A}]\{\dot{x}\} + \frac{1}{2}\rho U^2 Bk^2[\mathbf{B}]\{x\} \tag{8}$$

in which $[\mathbf{A}]$ and $[\mathbf{B}]$ are the matrices containing elements which consist of the coefficients H_i^* and A_i^* $(i = 1\text{–}4)$, length of the element, L_e and the width of the bridge deck. Note that $[\mathbf{A}]$ and $[\mathbf{B}]$ matrices are non-diagonal matrices, which have cross terms coupling between the torsional and vertical degrees of freedom.

By substituting equation (8) into equation (6), the final equation of motion can be expressed as

$$[\mathbf{M}]\{\ddot{x}\} + [\mathbf{C}]\{\dot{x}\} + [\mathbf{K}]\{x\} = \frac{1}{2}\rho U^2 B\left(\frac{k}{U}\right)[\mathbf{A}]\{\dot{x}\} + \frac{1}{2}\rho U^2 Bk^2[\mathbf{B}]\{x\}. \tag{9}$$

4.1. MULTIMODE FLUTTER ANALYSIS

In multimode analysis, the displacement vector $\{x\}$ is written in terms of modal matrix $[\mathbf{\Phi}]$ and modal co-ordinate vector $\{\xi(t)\}$ as

$$\{x\} = [\Phi]_{2n \times m}\{\xi(t)\}_{m \times 1} \tag{10}$$

where m is the number of modes considered. By using the mode superposition technique, the ith modal equation is derived from equation (9), can be written as

$$\ddot{\xi}_i(t) + \sum_{j=1}^{m}\left[\left(2\zeta_i\omega_i\delta_{ij} - \frac{1}{2}\rho U^2 B\frac{k}{U}\frac{d_{ij}}{\bar{m}_i}\right)\dot{\xi}_j(t)\right] + \sum_{j=1}^{m}\left[\left(\omega_i^2\delta_{ij} - \frac{1}{2}\rho U^2 Bk^2\frac{e_{ij}}{\bar{m}_i}\right)\xi_j(t)\right] = 0,$$
$$i = 1, 2, \ldots, m, \tag{11}$$

where δ_{ij} is the Kronecker delta function $= \begin{cases} 1 & : \quad i = j, \\ 0 & : \quad i \neq j, \end{cases}$ (12)

and d_{ij} and e_{ij} are the elements of the matrices $[\mathbf{D}]$ and $[\mathbf{E}]$ defined as

$$[\mathbf{D}] = [\mathbf{\Phi}]^{\mathrm{T}}[\mathbf{A}][\mathbf{\Phi}] \quad \text{and} \quad [\mathbf{E}] = [\mathbf{\Phi}]^{\mathrm{T}}[\mathbf{B}][\mathbf{\Phi}]. \tag{13}$$

Equation (11) can be written in a matrix form as

$$[\mathbf{I}]\{\ddot{\xi}(t)\} + [\mathbf{P}]\{\dot{\xi}(t)\} + [\mathbf{Q}]\{\xi(t)\} = \{0\} \tag{14}$$

in which $[\mathbf{I}]$ is the identity matrix of order m; $[\mathbf{P}]$ and $[\mathbf{Q}]$ are the square matrices of size $m \times m$ for which the elements can be defined as

$$P_{ij} = 2\zeta_i \omega_i \delta_{ij} - \frac{1}{2}\rho U^2 B \frac{k}{U}\frac{d_{ij}}{\bar{m}_i}, \tag{15}$$

$$q_{ij} = \omega_i^2 \delta_{ij} - \frac{1}{2}\rho U^2 B k^2 \frac{e_{ij}}{\bar{m}_i}, \tag{16}$$

By assuming

$$\xi_i(t) = a_i e^{i\omega t}, \quad i = \sqrt{-1}.$$

Equation (14) can be written as

$$[\mathbf{W}]_{m\times m}\{a\}_{m\times 1} = \{0\} \tag{17}$$

in which $\{a\} = \{a_1, a_2, \ldots, a_m\}^{\mathrm{T}}$ is the flutter mode shape vector, which indicates the relative participation of each structural mode in flutter, and the matrix $[\mathbf{W}]$ is given by

$$[\mathbf{W}] = \lfloor(\mathbf{Q} - \omega^2\mathbf{I}) + i(\omega\,\mathbf{P})\rfloor. \tag{18}$$

Equation (17) is the well-known eigenvalue problem. To satisfy the condition $\det[\mathbf{W}] = 0$, it is necessary that both the real and imaginary parts of the determinant be simultaneously zero [15]. This can be done by first fixing the value of reduced frequency, k, and seeking the value of ω, for which the determinant is zero, and repeating this procedure by changing the value of k until both parts of the determinant are zero at the same ω. By having the values of $\omega = \omega_f$ and $k = k_f$ for which $\det[\mathbf{W}] = 0$, the critical flutter speed can be evaluated as

$$U_f = \frac{B\omega_f}{k_f}. \tag{19}$$

5. RELIABILITY ANALYSIS AGAINST FLUTTER

The uncertainties in geometric and material properties of the bridge and the construction defects finally lead to uncertainties in the mass, stiffness and damping properties of the bridge. The other uncertainties that are considered include uncertainties in mathematical modelling and flutter derivatives. All these uncertainties affect the dynamic characteristics of the bridge and hence, the critical flutter speed (U_f). The uncertainties in mass and stiffness give rise to uncertainties in modal characteristic of the bridge and therefore, they are incorporated separately by a simulation procedure. The uncertainties arising from damping, mathematical modelling and flutter derivatives are considered directly in the reliability limit state function.

5.1. MASS AND STIFFNESS UNCERTAINTIES

The variation in the material and geometric properties of the bridge leading to the variations of the mass and stiffness properties of the system is complex and difficult to appropriately consider in the reliability analysis. The problem requires the mass and stiffness properties of the structure to be modelled as random variables leading to the use of stochastic finite element analysis or simulation procedure. In order to keep the present reliability analysis procedure simple and to obtain a preliminary estimate of reliability, the variation of the mass and stiffness properties of the bridge are considered by writing these matrices in the following form:

$$[\mathbf{K}_\rho] = \rho_1 [\mathbf{K}], \tag{20}$$

$$[\mathbf{M}_\rho] = \rho_2 [\mathbf{M}] \tag{21}$$

in which $[\mathbf{K}]$ and $[\mathbf{M}]$ are the basic stiffness and mass matrices of the bridge, respectively, and are considered as deterministic; ρ_1 and ρ_2 are log-normally distributed random variable factors which represent the variability of stiffness and mass matrices. In order to make this variation more general, the factor ρ_1 itself can be considered as a combination of three factors i.e.,

$$\rho_1 = F_1 F_2 F_3 \tag{22}$$

in which F_1 represents the effect of variability of modulus of elasticity (E); F_2 represents the uncertainty resulting from the variation of shear modulus (G); and F_3 represents the uncertainty resulting from bridge geometry. All these factors are considered as independent log-normally distributed random variables with a mean value of unity. The coefficient of variation (COV) of ρ_1 can be evaluated as [22]

$$1 + \delta \rho_1^2 = (1 + \delta_{F1}^2)(1 + \delta_{F2}^2)(1 + \delta_{F3}^2), \tag{23}$$

where $\delta\rho_1$ is the COV of the ρ_1, δ_{Fi} are the COV of the factors F_i ($i = 1$–3).

Since some of the elements of the stiffness matrix contain the parameter "E", while other elements contain the parameter "G", the values of δ_{F1} and δ_{F2} may be considered as $0{\cdot}5\ \delta_E$ and $0{\cdot}5\ \delta_G$; δ_E and δ_G are the COV of the parameters E and G respectively. Thus, equation (23) can be written as

$$1 + \delta_{\rho 1}^2 = (1 + (0{\cdot}5\delta_E)^2)(1 + (0{\cdot}5\delta_G)^2)(1 + \delta_{F3}^2). \tag{24}$$

In a similar manner, $\delta\rho_2$ can be calculated, assuming that $\rho_2 = \mu F_3$ in which μ represents the variation of mass density of the material.

Since ρ_1 and ρ_2 are log-normally distributed random variables, mean values of these random variables can be related to their standard deviations. If the standard deviation and mean values of ρ_1 and ρ_2 are known, random value of ρ_1 and ρ_2 can be artificially generated. For each combination of ρ_1 and ρ_2, $[\mathbf{K}_\rho]$ and $[\mathbf{M}_\rho]$ matrices are obtained from equations (20) and (21), and the corresponding critical flutter speed is determined from equations (18) and (19). The mean and standard deviation of the critical flutter speeds thus obtained, are used for further computation.

5.2. DAMPING AND MODELLING UNCERTAINTIES

Flutter speed, which is calculated in the previous section, is multiplied by three factors F_4, F_5, and F_6, in order to take into account the uncertainties due to damping, modelling and

flutter derivatives. These uncertainty coefficients are again considered as independent log-normally distributed random variables, with mean value of unity.

There are very few data available from the measured structural damping of the suspension bridges, which show the damping variability. According to Davenport [23], the structural damping of the long-span suspension bridges can be expressed as

$$\zeta_\theta = \frac{c}{n}\,\mathbf{E}, \tag{25}$$

where ζ_θ is the torsional mode damping ratio to critical; n is structural frequency (Hz); c is the proportionality coefficient; $\mathbf{E}$ is a log-normally distributed random factor with mean value of unity and coefficient of variation being 0·40. Since the flutter speed of the suspension bridges changes with the damping ratio ζ_θ, the effect of the COV of the factor F_4 (δ_{F4}) on the flutter wind speed is investigated with the upper limit of δ_{F4} as 0·40.

As discussed in the beginning of section 3, an idealized model of the actual bridge has been used for the free vibration analysis. This idealization leads to some approximations in the analysis procedure. In addition to the uncertainties arising due to these approximations, some other uncertainties also arise due to other assumptions and simplifications made in the modelling. For example, conversion of continuum of an assemblage of discrete elements leads to the consideration of less number of degrees of freedom in the system, use of lumped mass matrix leads to improper representation of inertia effect of the system; numerical analysis procedure used may introduce some errors in the results. The uncertainty factor F_5 is, therefore, introduced to take care of the above uncertainties in addition to those approximations already made in idealizing the system model. The COV of the factor F_5 is taken as 0·10.

Factor F_6 accounts for the uncertainties arising from the insufficient knowledge of flutter derivatives. In this study, flutter derivatives are estimated from experimentally given curves by Scanlan and Tomko [24], which were measured under zero angle of attack and low-speed flow (laminar flow). Thus, the effects of actual turbulent wind flow and wind direction are not considered in the analysis. While the directional effect may be ignored because the flutter condition is generally expected for zero angle of attack, the effect of turbulence may be important. It is shown by Bucher and Lin [5] that the presence of turbulence could delay the flutter-type instability of a bridge. Therefore, the consideration of turbulence is expected to increase the reliability against flutter failure. However, consideration of turbulence in the flutter analysis is very difficult, since it is quite often modelled as a weakly stationary process which requires random vibration and stochastic stability analyses to be performed. As a consequence, the turbulence effect is also neglected here, and the conventional futter failure is considered as reported in most literature (e.g., reference [15]). In addition to the insufficient knowledge on flutter derivatives as mentioned above, experimental error and curve-fitting techniques introduce extra uncertainties for the values of flutter derivatives used in the analysis. According to a study [25], disparity between the results of flutter derivatives obtained under turbulent and laminar conditions, especially for A_2^*, for reduced velocities $U/(nB) < 12$ is of the order of 15%. Keeping the above in view, the COV for factor F_6 (δ_{F6}) is taken as 0·20.

5.3. EVALUATION OF RELIABILITY

In the reliability analysis the failure of the structure is defined as

$$g(\mathbf{X}) = R - S < 0. \tag{26}$$

In general, the variables R and S are called resistance and load effect of the system and are functions of a number of basic random variables. In this study, R and S may be written as

$$R = U_f F_4 F_5 F_6, \qquad S = \bar{U}, \tag{27}$$

where $\bar{U}$ is the annual maximum mean wind speed at the site which is a random variable following Gumbel type I distribution. To evaluate the probability of failure (p_f), the joint probability density function of the associated randon variables say, $X_1, X_2, \ldots, X_n$, must be known. Then p_f is calculated as

$$p_f = \underset{g<0}{\int\int\cdots\int} f_X(x_1, x_2, \ldots, x_n)\,\mathrm{d}x_1\,\mathrm{d}x_2 \cdots \mathrm{d}x_n \tag{28}$$

in which $f_x(x_1, x_2, \ldots, x_n)$ is the joint probability density function of $X_1, X_2, \ldots, X_n$. For most engineering problems $f_x(x_1, x_2, \ldots, x_n)$ is not explicitly known. In such cases, some simplifying assumptions are made. One of the widely used assumptions provide [26]

$$p_f = \int_{-\infty}^{+\infty} f_s(s) F_R(s)\,\mathrm{d}s \tag{29}$$

$$p_f = 1 - \int_{-\infty}^{+\infty} f_R(r) F_S(r)\,\mathrm{d}r \tag{30}$$

where f_S and f_R are the PDF, and F_S and F_R the CDF of the variables S and R respectively. The values of integrals in equations (29) and (30) usually must be computed numerically. In very few cases, the closed-form solutions of these integrals are available.

5.4. PROBABILISTIC DESCRIPTION OF THE MEAN WIND

The annual maximum mean wind velocity $\bar{U}$ at the site is the random variable S in equation (27). It depends upon the wind environment at the site. In this study, it is assumed that the mean wind velocity is defined at the height of the bridge deck and is perpendicular to the longitudinal axis of the bridge (consistent with the assumption that flutter derivatives are obtained only for zero angle of attack). The distribution of the annual maximum mean wind velocity $\bar{U}$ or S is required to obtain p_f given by equations (29) and (30). For the reliability analysis, the annual maximum mean wind velocity having a certain return period is considered. The distribution of the annual maximum mean wind speed is assumed to follow the type I extremal (largest) distribution which is also called Gumbel type I distribution. The probability density (PDF) and distribution (CDF) functions of the annual maximum mean wind can be expressed as follows:

$$f_u(\bar{U}) = \bar{\alpha} \exp[-\bar{\alpha}(\bar{U} - \bar{u}) - \exp\{-\bar{\alpha}(\bar{U} - \bar{u})\}], \quad -\infty \leqslant \bar{U} \leqslant +\infty, \tag{31}$$

$$F_u(\bar{U}) = \exp[-\exp\{-\bar{\alpha}(\bar{U} - \bar{u})\}], \qquad -\infty \leqslant \bar{U} \leqslant +\infty \tag{32}$$

in which $f_u(\bar{U})$ is the probability density function (PDF), and $F_u(\bar{U})$ is the probability distribution function (CDF). The parameters $\bar{u}$ (location) and $\bar{\alpha}$ (dispersion) are given by

$$\bar{U}_{mean} = \bar{u} + \frac{0{\cdot}5772}{\bar{\alpha}}, \tag{33}$$

$$\sigma^2 = \frac{\pi^2}{6\bar{\alpha}^2}, \tag{34}$$

where $\bar{U}_{mean}$ and σ are the mean and standard deviation of the annual maximum mean wind speed $\bar{U}$.

5.5. ESTIMATION OF THE STATISTICAL PARAMETERS OF THE MEAN WIND SPEED

The parameters $\bar{u}$ and $\bar{\alpha}$ are determined using the concepts of return period (T_p) and design wind speed (U_d). The return period is defined as the time interval between two successive statistically independent events. The return period, which sometimes is also called the mean recurrence interval, is defined as

$$T_p = \frac{1}{p} = \frac{1}{1 - F_u(U_d)} \tag{35}$$

in which U_d is the specified design wind speed; and p is the probability of annual maximum mean wind speed $\bar{U}$, exceeding U_d in any 1 year.

If U_d is the lifetime design wind speed, $[1 - F_u(U_d)]$ is the probability of the annual extreme wind speed exceeding the design value U_d. Hence, the probability of not exceeding U_d in the first m year is $[F_u(U_d)]^m$. So, the probability of at least one extreme wind speed (maximum mean wind speed) exceeding U_d in m years is

$$p_m = 1 - [F_u(U_d)]^m, \tag{36}$$

$$F_u(U_d) = [1 - p_m]^{1/m}, \tag{37}$$

where m is the lifetime of the structure, and p_m is the associated risk during its lifetime.

The characteristic wind speed for the limit state is defined in this study as the annual maximum mean wind speed with an estimated probability of exceedence of 5% (0·05) in a lifetime period of 50 years (50) of the structure. Based on this definition, substituting $m = 50$ and $p_{50} = 0{\cdot}05$ into equation (37), the computed design wind speed U_d becomes the characteristic wind speed for the limit state for the site. It is shown below that different combinations of mean and standard deviation of the annual maximum mean wind speed can provide the same design wind speed. Thus, different combinations of the parameters $\bar{\alpha}$ and $\bar{u}$ can exist for the same design wind speed. By substituting the Gumbel distribution of $F_u(U_d)$ from equation (32), into equation (37), it can be written that

$$\exp[-\exp\{-\bar{\alpha}(U_d - \bar{u})\}] = [1 - p_m]^{1/m}. \tag{38}$$

Taking the log of both sides of this equation, it may be rewritten as

$$\exp\{-\bar{\alpha}(U_d - \bar{u})\} = S_1 \tag{39}$$

in which

$$S_1 = -\frac{1}{m}\ln(1 - p_m). \tag{40}$$

Again, taking the log of both sides of equation (39) and rearranging it, the following expressions are obtained:

$$U_d = \frac{S_2}{\bar{\alpha}} + \bar{u}, \tag{41}$$

where

$$S_2 = -\ln S_1. \tag{42}$$

From equations (33) and (34), the Gumbel distribution parameter $\bar{u}$ can be written in terms of mean (U_{mean}) and standard deviation (σ) of annual maximum mean wind speed as

$$\bar{u} = U_{mean} - \frac{0{\cdot}5772\sigma}{1{\cdot}28255} = U_{mean} - 0{\cdot}45\sigma. \tag{43}$$

Finally, by substituting $\bar{u}$ from equation (43) into equation (41),

$$U_d = \sigma\left[\frac{S_2}{1{\cdot}28255} - 0{\cdot}45\right] + U_{mean}. \tag{44}$$

Equation (44) can be rewritten in a convenient form as

$$U_d = U_{mean}\,[1 + S_3\,COV] \tag{45}$$

in which

$$S_3 = \left[\frac{S_2}{1{\cdot}28255} - 0{\cdot}45\right] \quad \text{and} \quad COV = \frac{\sigma}{U_{mean}}. \tag{46}$$

From equation (45), it is evident that different values of U_{mean} and COV can provide the same design wind speed U_d, as mentioned before. Thus, for a chosen set of values for m and p_m, U_d and U_{mean}, a value of COV and hence, a combination of parameters $\bar{\alpha}$ and $\bar{u}$ can be calculated from equations (46) and (33) and (34).

5.6. DISTRIBUTION OF THE RESISTANCE R OF THE SYSTEM

As mentioned earlier, the resistance of the structure R, (equation (27)) is defined as

$$R = U_f F_4 F_5 F_6 \tag{47}$$

in which all F_is are considered as independent log-normally distributed random variables. If it is now assumed that U_f is also log-normally distributed, then R will also be a log-normally distributed random variable having

$$\tilde{R} = \tilde{U}_f \tilde{F}_4 \tilde{F}_5 \tilde{F}_6, \tag{48}$$

$$1 + \delta_R^2 = (1 + \delta_{Uf}^2)(1 + \delta_{F4}^2)(1 + \delta_{F5}^2)(1 + \delta_{F6}^2), \tag{49}$$

$$\sigma_{In\,R}^2 = \ln(1 + \delta_R^2) \tag{50}$$

in which hat over script denotes the median values; δ is the coefficient of variation and σ_{InR} is the standard deviation of $\ln R$. The PDF of R can be obtained as

$$f_R(r) = \frac{1}{r\sigma_{InR}\sqrt{2\pi}} \exp\left[-\frac{1}{2}\left\{\frac{\ln\left(\dfrac{r}{\tilde{R}}\right)}{\sigma_{InR}}\right\}^2\right], \quad r > 0. \tag{51}$$

The above assumption leads to considerable ease in computational effort.

If the distribution of U_f is not assumed as log-normal, then $f_R(r)$ is numerically calculated. In this case, PDF of R can be written as [26]

$$f_R(r) = \int_{-\infty}^{\infty} \left| \frac{1}{f} \right| f_{Uf}\left(\frac{r}{f}\right) f_F(f)\,\mathrm{d}f, \tag{52}$$

where factor F is the product of factors F_4, F_5 and F_6; f_{Uf} and f_F are the PDFs of the flutter speed (U_f) and factor F respectively. It is assumed that the random variables F and U_f are independent. In equation (52), noting that f is a positive value and, by choosing $r/f = X$, equation (52) can be expressed as

$$f_R(r) = \int_0^{\infty} \frac{1}{X} f_{Uf}(X)\ f_F\left(\frac{r}{X}\right) \mathrm{d}X. \tag{53}$$

Assuming that F is log-normally distributed, the reliability of the bridge for actual distribution of the flutter speed U_f is numerically calculated using equation (53). Reliability estimates using $f_R(r)$ calculated by both equations (51) and (53) are obtained and compared in the numerical study.

6. NUMERICAL STUDIES

As a numerical example, the Vincent Thomas Suspension Bridge located between San Pedro and Terminal Island in Los Angeles County, California was chosen. For this three-span suspension bridge, the structural data are given by Abdel-Ghaffar [20, 21].

The stiffening girder is assumed to be hinged at the ends of each span, and the cables are free to move at the tower top (i.e., roller-type cable connection). The number of elements in the side spans, $N_1 = N_3$, was taken to be 11 elements, and those for the center span, N_2 was taken as 28 elements.

Flutter derivatives H_i^* and A_i^*, $i = 1$–3 are taken from Scanlan and Tomko [24]. The approximate theoretical expressions for the flutter derivatives may be written as

$$\begin{aligned}
&A_1^* \simeq 0, \quad H_1^* = -0{\cdot}8\ y \quad \text{for all } y\\
&A_2^* = -0{\cdot}1436 \sin(0{\cdot}5984\, y), \quad 0 \leqslant y \leqslant 5{\cdot}25,\\
&A_2^* = 0{\cdot}08422y - 0{\cdot}4411, \quad 5{\cdot}25 < y,\\
&H_2^* = 0, \quad 0 \leqslant y \leqslant 5,\\
&H_2^* = 0{\cdot}00582\ y^3 - 0{\cdot}0121\ y^2 - 0{\cdot}60252, \quad 5 < y,\\
&A_3^* = 0, \quad 0 \leqslant y \leqslant 2,\\
&A_3^* = 0{\cdot}2y - 0{\cdot}4, \quad 2 \leqslant y \leqslant 6,\\
&A_3^* = 0{\cdot}3y - 1, \quad 6 < y,\\
&H_3^* = 0, \quad 0 \leqslant y \leqslant 4,\\
&H_3^* = -0{\cdot}011666\ y^3 + 0{\cdot}11\ y^2 - 1{\cdot}41334\ y + 4{\cdot}64003, \quad 4 < y
\end{aligned} \tag{54}$$

in which $y = 2\pi/k$; $k = B\omega/U$.

Since the values of H_4^* and A_4^* for this bridge are not available, it is assumed to be negligible. The given approximate theoretical values of flutter derivatives are plotted in Figure 3.

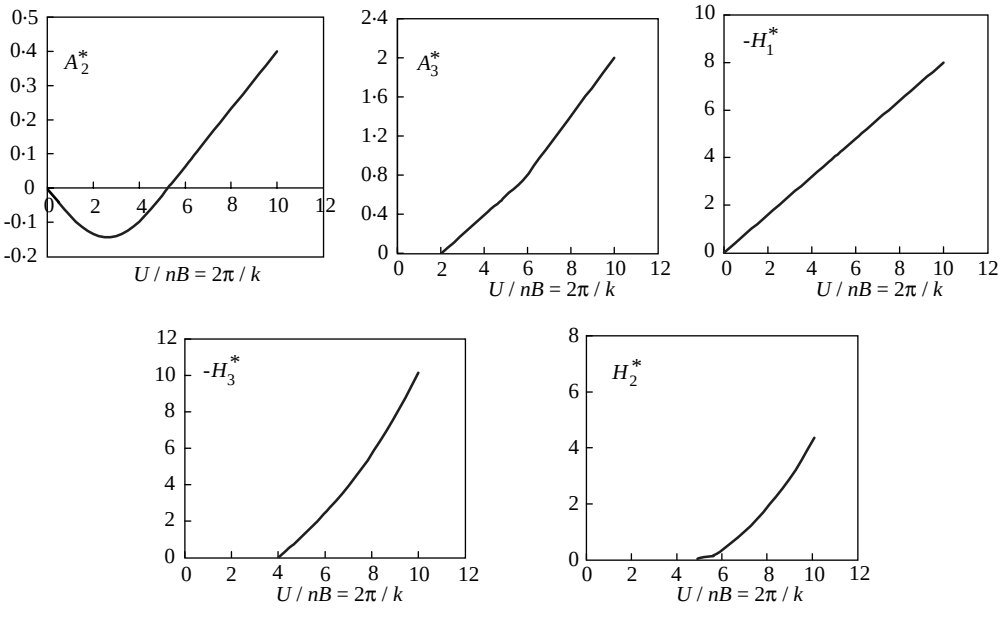

Figure 3. Approximate flutter derivatives (equation (54)) of Thomas Suspension Bridge.

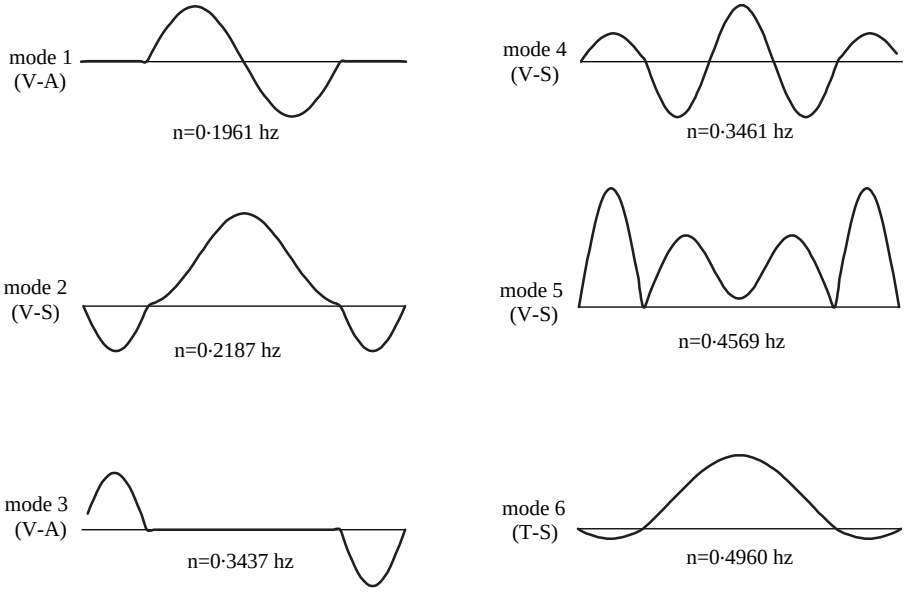

Figure 4. First six free vertical and torsional vibrations mode shapes.

6.1 FREE VIBRATION

The results of the free vibrational analysis (first 19 frequencies and first 6 mode shapes) are shown in Figure 4 and Table 1. In the figure, V and T refer to vertical and torsional, respectively, and A and S refer to anti-symmetric and symmetric respectively. It is seen that

TABLE 1

Modal properties of Thomas Suspension Bridge

Mode number	Natural frequency (Hz)	Frequency ω (rad/s)	Mode type	Modal mass ($\bar{m}$)
1	0·1961	1·2324	V–AS	2461656·04
2	0·2187	1·3743	V–S	2242256·44
3	0·3437	2·1595	V–AS	1694918·34
4	0·3461	2·1744	V–S	2839954·34
5	0·4569	2·8710	V–S	2476722·50
6	0·4960	3·1163	T–S	97979869·71
7	0·5445	3·4215	V–AS	2596112·11
8	0·7023	4·4124	T–AS	104379722·40
9	0·7960	5·0012	V–S	2381936·85
10	1·0632	6·68024	T–AS	71796835·18
11	1·0725	6·7388	T–S	127301319·14
12	1·0878	6·8351	V–AS	854013·18
13	1·0879	6·8352	V–S	1112550·47
14	1·0948	6·8791	V–AS	2476727·02
15	1·1229	7·0556	T–S	90565331·63
16	1·4493	9·1062	V–S	2463948·43
17	1·4709	9·2418	T–AS	109804780·28
18	1·8551	11·6557	V–AS	2617732·09
19	1·9000	11·9381	T–S	103247913·56

Note: T = torsional; V = vertical; S = symmetric; AS = anti-symmetric.

the first five modes correspond to the vertical mode of vibration. Note that free vibrational mode shapes are either purely vertical or purely torsional as it would be expected.

6.2. FLUTTER

In order to study the participation of different modes in the flutter contribution, the flutter speed is evaluated by multimode analysis by considering the original values of mass and stiffness properties by taking ρ_1 and ρ_2 as unity. Table 2 shows the results for five cases, which include different number of modes considered in the flutter analysis. For cases 1, 2 and 5, the magnitude of flutter mode shape $|a_i|$, which shows the relative contribution of any structural mode in flutter occurrence, is given in Table 3. It can be seen from Table 3 that the sixth mode (i.e., the first symmetric torsional mode) is the predominant mode for the flutter condition. This mode gets coupled with the second and fifth modes, which are the first and third vertical symmetric modes, respectively, for the flutter condition. The contributions of the other modes in flutter occurrence are very less in comparison with these modes. Therefore, the flutter condition was investigated by considering only the three modes namely second, fifth and sixth.

Since no strong coupling between the modes is observed for the bridge problem with flutter derivatives shown in Figure 3, it was decided to change the bridge deck configuration to that of an airfoil (keeping stiffness and mass properties same as the original deck) and reanalyze the system for flutter. The airfoil flutter derivatives, which are given by Jain *et al.* [15], are expressed in terms of Theodorsen's [27] circulation functions

TABLE 2

Flutter conditions evaluated by multimode analysis ($\zeta = 1\%$, $\rho_1 = 1$, $\rho_2 = 1$)

Case	No. of modes considered	Flutter frequency ω (rad/s)	Flutter reduced frequency k	Flutter speed (m/s)
1	6	2·855	0·93	57·01
2	7	2·855	0·93	57·01
3	8	2·855	0·93	57·01
5	10	2·855	0·93	57·01
9	19	2·855	0·93	57·01

TABLE 3

Relative flutter mode participation ($\rho_1 = 1$, $\rho_2 = 1$, $\zeta = 1\%$)

	Magnitude: $\lvert a_i \rvert$ Mode no.									
Case (ref. Table 2)	1	2	3	4	5	6	7	8	9	10
	$\times 10^{-7}$	$\times 10^{-2}$	$\times 10^{-18}$	$\times 10^{-4}$	$\times 10^{-1}$	$\times 1$	$\times 10^{-10}$	$\times 10^{-7}$	$\times 10^{-4}$	$\times 10^{-9}$
1	7·8630	8·2849	1·2820	7·0984	1·7827	1·0	—	—	—	—
2	8·7197	9·1670	3·0392	7·8965	1·9034	1·0	4·2003	—	—	—
3	7·8998	9·1670	1·7308	7·8965	1·9034	1·0	4·0899	9·1579	6·5869	2·2922

$C(k) = F(k) + \mathrm{i}\, G(k)$ as

$$H_1^* = -\frac{2\pi}{k} F(k), \quad A_1^* = \frac{\pi}{2k} F(k), \tag{55a}$$

$$H_2^* = -\frac{\pi}{k}\left[\frac{1 + F(k)}{2} + \frac{2G(k)}{k}\right], \quad A_2^* = \frac{\pi}{k}\left[\frac{F(k) - 1}{8} + \frac{G(k)}{2k}\right], \tag{55b}$$

$$H_3^* = -\frac{\pi}{k^2}\left[2F(k) - \frac{kG(k)}{2}\right], \quad A_3^* = \frac{\pi}{k^2}\left[\frac{F(k)}{2} - \frac{kG(k)}{8}\right], \tag{55c}$$

$$H_4^* = \frac{\pi}{2}\left[1 + \frac{4G(k)}{k}\right], \quad A_4^* = -\frac{\pi}{2k} G(k) \tag{55d}$$

and

$$F(k) = \frac{\mathrm{J}_1(k)[\mathrm{J}_1(k) + \mathrm{Y}_0(k)] + \mathrm{Y}_1(k)[\mathrm{Y}_1(k) - \mathrm{J}_0(k)]}{[\mathrm{J}_1(k) + \mathrm{Y}_0(k)]^2 + [\mathrm{Y}_1(k) - J_0(k)]^2}, \tag{55e}$$

$$G(k) = \frac{\mathrm{Y}_1(k)\,\mathrm{Y}_0(k) + \mathrm{J}_1(k) J_0(k)}{[\mathrm{J}_1(k) + \mathrm{Y}_0(k)]^2 + [\mathrm{Y}_1(k) - J_0(k)]^2}. \tag{55f}$$

in which J_0 and J_1 are Bessel functions of the first kind; and Y_0 and Y_1 are Bessel functions of the second kind. Since for Thomas Suspension Bridge the values of H_4^* *and* A_4^* are not

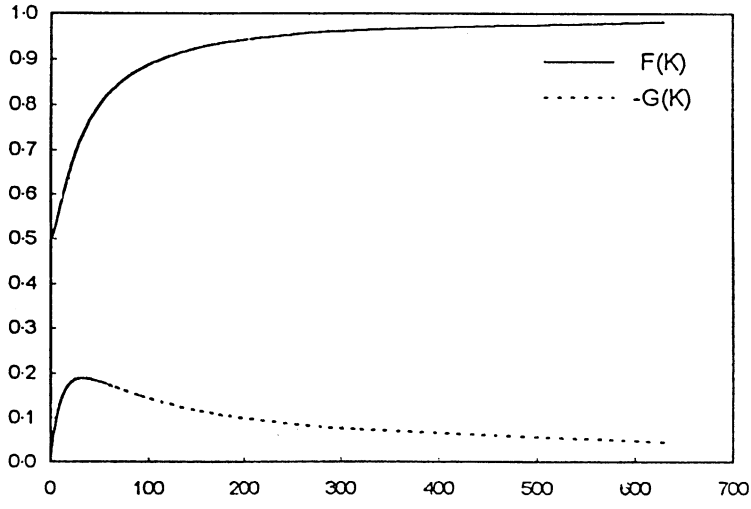

Figure 5. Theodorson's circulation function.

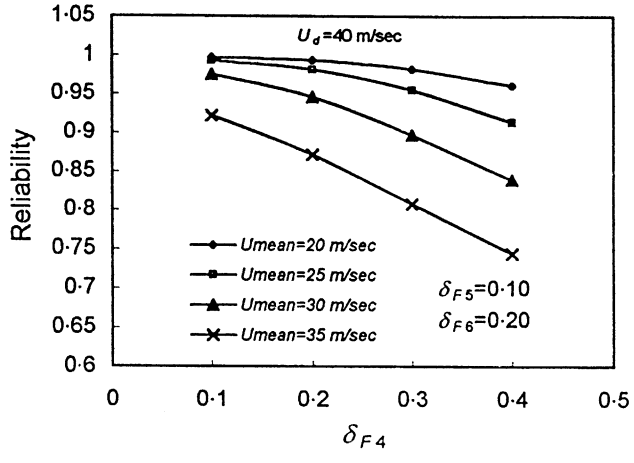

Figure 6. Effect of coefficient of variation of damping factor (δ_{F4}) on reliability.

available, for consistency H_4^* and A_4^* are neglected here. Functions $F(k)$ and $G(k)$ are plotted in Figure 5. It is observed that in this case, only the second and sixth modes get coupled; and the flutter speed is 116·17 m/s at a flutter frequency $\omega = 2{\cdot}074$ rad/sec and $k = 0{\cdot}322$. Magnitudes of the flutter modes are $|a_2| = 1{\cdot}13$ and $|a_6| = 1{\cdot}0$. Thus, a significant coupling between the two modes is observed for this case.

6.3. RELIABILITY ESTIMATE

Flutter speed was obtained for 42 sets of ρ_1 and ρ_2 (equations (20) and (21)). For each set, the mean value of the modal damping was taken as 0·6% and the flutter derivatives were taken from Figure 3. The combination of different values of ρ_1 and ρ_2 are considered such that the maximum dispersion in critical flutter speed, U_f, can be obtained. The mean (μ_{Uf}),

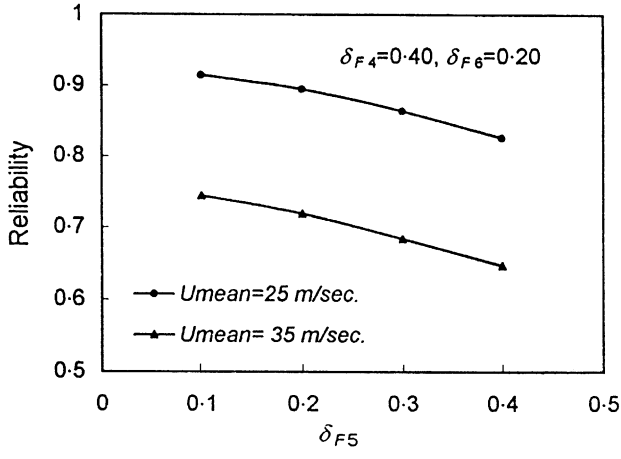

Figure 7. Effect of coefficient of variation of modelling (δ_{F5}) on reliability.

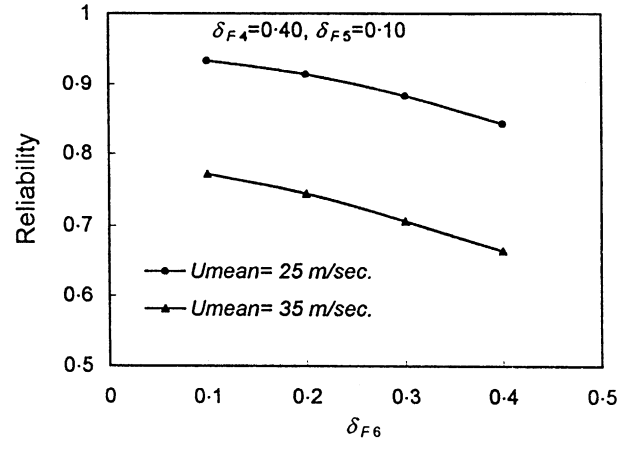

Figure 8. Effect of coefficient of variation of flutter derivatives (δ_{F6}) on reliability.

standard deviation (σ_{Uf}) and coefficient of variation (δ_{Uf}) of the flutter speed as obtained from 42 runs are 52·25 m/s, 4·4149 m/s and 8·45% respectively. Choosing $m = 50$ years as lifetime of the bridge and $p_m = 5\%$ as the risk of the failure within 50 years, the reliability of the bridge against flutter failure is carried out. For the reliability analysis, the mean values of the factors F_4, F_5 and F_6 are taken as unity and the coefficients of variation δ_{F4}, δ_{F5} and δ_{F6} are initially taken as 0·40, 0·10 and 0·20 respectively. The sensitivity of the parameters δ_{F4}, δ_{F5} and δ_{F6} on the reliability estimate is studied separately and is shown in Figures 6–8. The design wind speed is considered as $U_d = 40$ m/s.

As mentioned before, the reliability estimates obtained by assuming U_f to be log-normally distributed (equation (51)) provide ease in computational effort. For the design wind speed of 40 m/s, the reliability estimates are obtained by considering the actual distribution of U_f (equation (53)) and are compared with those obtained by assuming U_f to be log-normally distributed (Table 4). It is seen that the difference between the two results is not much. Thus, for the ease of computation it is accepted to treat U_f as log-normally distributed.

TABLE 4

Effect of flutter wind speed distribution on reliability ($U_d = 40\,m/s$; $\delta_{F4} = 0{\cdot}20$, $\delta_{F5} = 0{\cdot}10$, $\delta_{F6} = 0{\cdot}20$, $\zeta = 0{\cdot}6\%$, $m = 50$, $p_m = 5\%$)

Distribution of U_f	Mean wind speed (m/s)			
	20	25	30	35
Log-normal	0·9866	0·9722	0·9371	0·8670
Actual distance	0·9784	0·9626	0·9241	0·8486

TABLE 5

Results of the reliability analysis for $U_d = 40\,m/s$ ($m = 50$, $p_m = 5\%$)

Parameters	Mean wind (m/s)			
	20	25	30	35
COV	0·20342	0·12205	0·006678	0·02906
$\bar{\alpha}$	0·31525	0·42034	0·63034	1·26103
$\bar{u}$	18·1691	23·6268	29·0845	35·5423
R_0 (reliability)	0·9612	0·9142	0·8391	0·7441

Note: $\bar{\alpha}$ and $\bar{u}$ are the Gumbel distribution parameters.

For different combinations of coefficient of variation and mean wind speed at the site having the same design wind speed (equation (45)), the reliability estimates are obtained. Table 5 shows the reliability of the bridge against flutter failure. It is seen that for the same design wind speed, the reliability varies significantly with the values of the annual maximum mean wind speed (U_{mean}) assumed for computing the parameters ($\bar{u}$ and $\bar{\alpha}$) of the Gumbel distribution of the wind speed at the site (equation (45)). Higher the value of the assumed U_{mean} (and hence, $\bar{u}$ and $\bar{\alpha}$) lower is the value of the reliability. Thus, the reliability against flutter failure for suspension bridges designed for the same design wind speed could be different for different locations. For higher values of location ($\bar{u}$) and dispersion ($\bar{\alpha}$) parameters, the reliability estimates are lower.

6.4. EFFECT OF DAMPING FACTOR ON RELIABILITY

Figure 6 shows the effect of the coefficient of variation of the damping factor (F_4) on the reliability estimate for a design wind speed (U_d) of 40 m/s. The reliability decreases with the increase in the coefficient of variation of the damping factor (δ_{F4}). For higher values of U_{mean}, the rate of decrease in reliability with the increase in δ_{F4} is more.

6.5. EFFECTS OF FACTORS F_5 AND F_6 ON RELIABILITY

Figures 7 and 8 show how the reliability decreases with the increase in the coefficients of variation of the factors F_5 (modelling) and F_6 (flutter derivatives). The results are shown for

two values of U_{mean} keeping the design wind speed (U_d) same. It is seen that the rate of decrease of reliability remains the same for both values of U_{mean}.

7. CONCLUSIONS

The reliability of suspension bridges against flutter failure is investigated. The reliability is estimated for uncertainties in stiffness and mass properties, modelling, damping and flutter derivatives of the deck cross-section of the bridge. All uncertainty factors are assumed to be log-normally distributed. The annual maximum mean wind speed at the site is assumed to follow Gumble type I distribution. Using the proposed method of analysis, the results of the study on the Vincent Thomas Suspension Bridge show that (1) the flutter wind speed may be assumed to be log-normally distributed without introducing much error in the reliability estimate; (2) the reliability of suspension bridges designed for the same n-year wind speed may significantly vary depending upon the prevailing annual maximum mean wind speed at the location of the bridge; (3) the coefficient of variation of damping factor may significantly decrease the reliability estimate for higher values of the mean annual maximum wind speed; (4) coefficients of variation of multiplying factors associated with modelling and flutter derivatives can have an appreciable effect on the reliability estimate.

REFERENCES

1. A. G. DAVENPORT 1961 *Quarterly Journal of the Royal Meteorological Society* **87**, 194–211. The spectrum of horizontal gustiness of near the ground in high winds.
2. A. G. DAVENPORT 1962 *Journal of Structural Division, American Society of Civil Engineers* **88**, 233–268. Buffeting of a suspension bridge by storm winds.
3. Y. K. LIN 1979 *Journal of the Engineering Mechanics Division, American Society of Civil Engineers* **105**, 921–932. Motion of suspension bridge in turbulent winds.
4. R. H. SCANLAN and H. GADE 1977 *Journal of the Structural Division, American Society of Civil Engineers* **103**, 1867–1883. Motion of suspension bridge spans under gusty wind.
5. C. G. BUCHER and Y. K. LIN 1988 *Journal of the Engineering Mechanics Division, American Society of Civil Engineers* **114**, 2055–2071. Stochastic stability of bridges considering coupled modes.
6. Y. NAKAMURA and T. YOSHIMURA 1976 *Journal of the Engineering Mechanics Division, American Society of Civil Engineers* **102**, 685–700. Binary flutter of suspension bridge deck sections.
7. R. H. SCANLAN and N. P. JONES 1990 *Journal of Structural Division, American Society of Civil Engineers* **116**, 279–297. Aeroelastic analysis of cable-stayed bridges.
8. Z. Q. CHEN 1994 *Proceedings of the Symposium on Cable-Stayed Bridges, Shanghai, China*, 10–13. The three dimensional analysis of behaviours investigation on the critical flutter state of bridges.
9. N. P. JONES and R. H. SCANLAN 1991 *Infrastructure '91, International Workshop on Technology for Hong Kong's Infrastructure Development*, 281–290. Hong Kong: Commercial Press. Issues in the multimode aeroelastic analysis of cable-stayed bridges.
10. A. NAMINI, P. ALBRECHT and H. BOSCH 1992 *Journal of Structural Division, American Society of Civil Engineers* **118**, 1509–1526. Finite element-based flutter analysis of cable-suspended bridges.
11. Y. K. LIN and J. N. YANG 1983 *Journal of Engineering Mechanics Division, American Society of Civil Engineers* **109**, 586–603. Multimode bridge response to wind excitation.
12. H. TANAKA, N. YAMAMURA and N. SHIRASHI 1993 *Journal of structural Mechanics and Earthquake Engineering, Japanese Society of Civil Engineers* **10,** 35–46. Multi-mode flutter analysis and two and three dimensional model tests on bridges with non-analogous modal shapes.
13. T. MIYATA, K. TADA, H. SATO, H. KATSUCHI and Y. HIKAMI 1994 *Proceedings Symposium on Cable-Stayed and Suspension Bridges*, 163–170. Deauville, France: Association Française pour la Construction. New findings of coupled-flutter in full model wind tunnel tests on the Akashi Kalikyo Bridge.
14. T. MIYATA 1995 *State of the Art in Wind Engineering, Ninth International Conference on Wind Engineering, New Delhi*, 249–280. Full model testing of large cable-stayed bridges.

15. A. JAIN, N. P. JONES and R. H. SCANLAN 1996 *Journal of Structural Engineering, American Society of Civil Engineers* **122**, 716–725. Coupled flutter and buffeting analysis of long-span bridges.
16. H. KATSUCHI, N. P. JONES and R. H. SCANLAN 1999 *Journal of Structural Engineering, American Society of Civil Engineers* **125**, 60–70. Multimode coupled flutter and buffeting analysis of the Akashi-Kaikyo Bridge.
17. S. MALA 1988 *A Thesis of Master of Engineering, Asian Institute of Technology, AIT, Bangkok, Thailand*. Safety and reliability of the cable system of a cable-stayed bridge under stochastic earthquake loading.
18. H. O. MADSEN and P. O. ROSENTHAL 1992 *Proceedings of the International Symposium on Aerodynamics of Large Bridges, Copenhagen, Denmark*, 19–21 *February*, 33–43. Wind criteria for long span bridges.
19. M. ABDEL-GHAFFAR and L. I. RUBIN 1984 *Journal of Engineering Mechanics, American Society of Civil Engineers* **110**, 1467–1484. Torsional earthquake response of suspension bridges.
20. A. M. ABDEL-GHAFFAR 1980 *Journal of the Structural Division, American Society of Civil Engineers* **106**, 2053–2074. Vertical vibration analysis of suspension bridges.
21. A. M. ABDEL-GHAFFAR 1979 *Journal of the Structural Division, American Society of Civil Engineers* **105**, 767–789. Free torsional vibrations of suspension bridges.
22. COMMITTEE ON FATIGUE AND FRACTURE RELIABILITY 1982 *Journal of the Structural Division, American Society of Civil Engineers* **108**, 47–69. Fatigue reliability: variable amplitude loading.
23. G. DAVENPORT and G. LAROSE 1989 *Presented at the Canada–Japan Workshop on Bridge Aerodynamics, Ottawa, Canada*, 25–27. The structural damping of long span bridges: an interpretation of observation.
24. R. H. SCANLAN and J. J. TOMKO 1971 *Journal of the Engineering Mechanics Division, American Society of Civil Engineers* **97**, 1717–1737. Airfoil and bridge deck flutter derivatives.
25. E. SIMIU and R. H. SCANLAN 1986 *Wind Effects on Structures*. New York: John Wiley & Sons, Inc., second edition.
26. R. RANGANATHAN 1990 *Reliability Analysis and Design of Structures*. New Delhi: McGraw-Hill.
27. T. THEODORSEN 1935 *NACA Report* 496, *U.S. National Advisory committee for Aeronautics, Langley, VA*. General theory of aerodynamic instability and the mechanism of flutter.